Robust Design Optimization of Electrical Machines: Multi-objective Approach

Gang Lei, *Member, IEEE*, Gerd Bramerdorfer, *Senior Member, IEEE*, Bo Ma, Youguang Guo, *Senior Member, IEEE*, and Jianguo Zhu, *Senior Member, IEEE*

***Abstract*—This paper presents a new method for multi-objective robust design optimization of electrical machines and provides a detailed comparison with so far introduced techniques. First, two robust design approaches, worst-case design and design for six-sigma, are compared with the conventional deterministic approach for multi-objective optimization. Through a case study on a permanent magnet motor, it is found that the reliabilities of motors produced based on robust designs are 100% under the investigated constraints, while the reliabilities of deterministic designs can be lower than 30%. A major disadvantage of robust optimization is the huge computation cost, especially for high-dimensional problems. To attempt this problem, a new multi-objective sequential optimization method (MSOM) with an orthogonal design technique and hypervolume indicator (as a measure of convergence) is proposed for both deterministic and robust design optimization of electrical machines. Through another case study, it is found that the new MSOM can improve motor performance and greatly reduce the computational cost. For the robust optimization, the number of required finite element simulations can be reduced by more than 40%, compared with that required by the conventional approach. The proposed method can be applied to many-objective (robust) design optimization of electrical machines.**

***Index Terms*—Electrical machines, manufacturing tolerances, multi-objective optimization, orthogonal design, permanent magnet motor, robust design, sequential optimization method.**

I. Introduction

DESIGN optimization of electrical machines is a multi-objective and multiphysics problem, which usually includes electromagnetic analysis, thermal analysis, stress and modal analysis [1-6]. The objectives always conflict with each other, such as minimizing the material cost and maximizing the output power. The optimal solutions are normally called as non-dominated or non-inferior solutions and are illustrated as a Pareto front. To efficiently derive the optimal designs, a number of multi-objective optimization algorithms developed in the field of evolutionary computation, like multi-objective genetic algorithm (MOGA), have been applied to the design optimization of various electrical machines, such as permanent magnet (PM) motors and reluctance synchronous machines [7-15].

There are two main types of design models for the multi-objective optimization of electrical machines, deterministic and robust models. The main difference is that there is no uncertainty information, like material diversities and manufacturing tolerances of PMs, in the deterministic model. The obtained optimal deterministic designs can be very impressive theoretically, but the practical performance of the motor after production may be significantly different due to the unavoidable uncertainties in the manufacturing process, which will result in unacceptable failure rate in production [2,16,17]. In this context, robust design optimization has been introduced to the (multi-objective) optimization of electrical machines.

Regarding the robust design of electrical machines, there are three popular approaches, the Taguchi parameter design [18-20], worst-case (WC) design [21,22], and design for six-sigma (DFSS) [16,17,23]. WC and DFSS can be easily converted into multi-objective situations. However, it is hard to convert the Taguchi parameter design into a multi-objective optimization problem due to the special formulation of the method. Thus, WC and DFSS will be investigated and compared with the deterministic multi-objective approach in this work.

A major challenge for the robust (multi-objective) optimization of electrical machines is the huge computation cost, especially in the high-dimensional situation. It originates from two aspects, multiphysics analysis like finite element model (FEM) for the electromagnetic analysis, and robustness evaluation of a design candidate, for example, realized by applying Monte Carlo analysis (MCA) [2,16]. To attempt this challenge, a new multi-objective sequential optimization method (MSOM) is proposed for both deterministic and robust multi-objective optimization problems in this work. An orthogonal design method and a hypervolume indicator used as a measure of convergence are employed in the new method to improve its efficiency. To illustrate the effectiveness of the proposed method, a case study will be investigated.

G. Lei, B. Ma, and Y. Guo are with the School of Electrical and Data Engineering, University of Technology Sydney, Ultimo, NSW 2007, Australia (email: gang.lei@uts.edu.au). Corresponding author: Bo Ma.

G. Bramerdorfer is with the Department of Electrical Drives and Power Electronics, Johannes Kepler University Linz, Linz 4040, Austria (email: gerd.bramerdorfer@jku.at)

J. Zhu is with the School of Electrical and Information Engineering, University of Sydney, Camperdown, NSW 2006, Australia.

The remainder of this paper is organized as follows. Section II briefs the formulations of a deterministic and two robust multi-objective design optimization models. Section III describes the design example, a PM motor with soft magnetic composite (SMC) cores, and specifies the uncertainty information. Section IV presents a comparative study of these multi-objective design optimization methods based on the design example. Section V describes the proposed new MSOM for the high-dimensional multi-objective design optimization problems. Section VI gives a detailed comparison of the results and a consequent discussion to show the effectiveness of the proposed method, followed by the conclusion.

II. Multi-objective Robust Design Optimization Methods

A typical multi-objective optimization model of a deterministic optimization problem can have the form as

$$\begin{aligned} \min:\quad & \{f_i(\mathbf{x}), i = 1,2,\dots,p\} \\ \text{s.t.}\quad & g_j(\mathbf{x}) \le 0, j = 1,2,\dots,m \\ & \mathbf{x}_l \le \mathbf{x} \le \mathbf{x}_u \end{aligned} \tag{1}$$

where p and m are the numbers of objectives, $f_i(\mathbf{x})$, and constraints, $g_j(\mathbf{x})$, respectively, $\mathbf{x}$ is a vector, and its size corresponds to the number of design parameters considered. Any design investigated features a particular setting of x. By analogy, x_l and $\mathbf{x}_u$ are vectors of the lower and upper boundaries of all design parameters, and thus they are of the same size as $\mathbf{x}$. In this model, $\mathbf{x}$ does not include any uncertainty information, like manufacturing tolerances.

Through extensive research activity, it is found that there are many uncertainties in the practical manufacturing process of electrical machines, such as material diversities (like different remanences of a batch of PMs), manufacturing tolerances (like the variations of dimensions of a batch of PMs and the lengths of air gap of a batch produced PM motors), and assembly imperfections (for example, the eccentricity problem) [24-29]. These uncertainties will affect the practical performance of the produced electrical machines, for example, the cogging torque and torque ripple may be significantly higher than the value obtained by finite element simulations for the ideal geometry [24,25]. To consider the uncertainties and reduce their impact on the motor performance in the production, two robust design approaches have been investigated for the multi-objective optimization of electrical machines, the WC design and DFSS [2,21-23].

Regarding the WC robust design approach, its multi-objective optimization model can be defined as

$$\begin{aligned} \min:\quad & \{f_{w,i}(\mathbf{x}) = \max_{\boldsymbol{\xi}\in U(\boldsymbol{\xi})} f_i(\mathbf{x},\boldsymbol{\xi}), i = 1,2\dots,p\} \\ \text{s.t.}\quad & g_{w,j}(\mathbf{x}) = \max_{\boldsymbol{\xi}\in U(\boldsymbol{\xi})} g_j(\mathbf{x},\boldsymbol{\xi}) \le 0, j = 1,2,\dots,m \\ & U(\boldsymbol{\xi}) = \{\boldsymbol{\xi} \in R^k \,||\boldsymbol{\xi} - \boldsymbol{\xi}_n| \le \Delta\boldsymbol{\xi}\} \end{aligned} \tag{2}$$

where $\boldsymbol{\xi}$ and $\boldsymbol{\xi}_n$ stand for the vector and nominal values of noise factors, respectively, $U(\boldsymbol{\xi})$ represents the uncertainty range of these parameters. Similar to the single-objective scenario, WC multi-objective model is a minimax optimization problem. It uses the worst motor performance of a design under uncertainties as a measure of robustness. Thus, a WC-designed motor can have very high reliability in production.

For the DFSS robust design approach, its multi-objective optimization model can be expressed as

$$\begin{aligned} \min:\quad & \{F_i[\mu_f(\mathbf{x}), \sigma_f(\mathbf{x})], i = 1,2,\dots,p\} \\ \text{s.t.}\quad & g_j[\mu_f(\mathbf{x}), \sigma_f(\mathbf{x})] \le 0,\ j = 1,2,\dots,m \\ & \mathbf{x}_l + n\boldsymbol{\sigma}_\mathbf{x} \le \boldsymbol{\mu}_\mathbf{x} \le \mathbf{x}_u - n\boldsymbol{\sigma}_\mathbf{x} \\ & \text{LSL} \le \mu_f \pm n\sigma_f \le \text{USL} \end{aligned} \tag{3}$$

where μ and σ are the mean and standard deviation (SD), respectively, and they are usually estimated by Monte Carlo analysis (MCA) method. LSL and USL are the lower and upper specification limits, respectively. n is the sigma level, and it is defined as 6 in many applications. The value of n can be equivalent to a probability of a normal distribution. For example, 6σ is equivalent to 0.002 (or a per cent of pass 99.9999998%) and 3.4 defects per million opportunities (DPMO) in terms of short-term and long-term quality control, respectively [2,30].

The main difference between WC and DFSS approaches is the requirement of probability distribution functions of the uncertainty parameters. WC approach only needs the variation range of these parameters, while DFSS usually requires probability distribution functions for all uncertain parameters and normal distributions are widely employed in DFSS.

To compare the motor's reliability by using different design approaches, a criterion called as probability of failure (PoF) will be used in this work [2,30]. It has the form as

$$\text{PoF} = 1 - \prod_{i=1}^{m} P(g_i \le 0) \tag{4}$$

III. Description of the Case Scenario

This section describes an exemplary optimization problem that is applied to compare the performance of the three multi-objective optimization methods introduced in Section II. The comparison results will be shown in the next section.

Figure 1 shows a 3-D design structure and parameters of the investigated motor, a PM claw pole motor (CPM) with SMC stator and NdFeB magnets. Table I lists seven main design parameters (as well as optimization parameters), for this motor. The rated output power and efficiency of the reference motor are 500 W and 81.5%, respectively. More details of this motor can be found in [31-33]. For the multi-objective optimization of this motor, the two selected objectives are minimizing the material cost (*Cost*) and maximizing the output power (P_{out}). The deterministic multi-objective optimization model can be defined as

$$\begin{aligned} \min:\quad & \begin{cases} f_1(\mathbf{x}) = Cost \\ f_2(\mathbf{x}) = 1000 - P_{out} \end{cases} \\ & g_1(\mathbf{x}) = 500 - P_{out} \le 0 \\ & g_2(\mathbf{x}) = 0.815 - \eta \le 0 \\ \text{s.t.}\quad & g_3(\mathbf{x}) = sf - 0.7 \le 0 \\ & g_4(\mathbf{x}) = T_{coil} - 75 \le 0 \\ & g_5(\mathbf{x}) = T_{pm} - 75 \le 0 \\ & \mathbf{x}_l \le \mathbf{x} \le \mathbf{x}_u \end{aligned} \tag{5}$$

where η, sf, T_{coil}, and T_{pm} are the motor efficiency, slot filling factor, temperature rise in the winding, and temperature rise in the PM, respectively. Thus, this model requires both electromagnetic and thermal analyses. For this purpose, a 3-D FEM and a 3-D thermal network model are used [2,32,33].

Table II lists several calculated and measured motor performance parameters, including the back EMF constant, no-load core loss and temperature rise in winding [32,33]. As shown, the calculated and measured values are in good agreement. Thus, it is reliable to use these models to conduct the following multi-objective optimization for this motor.

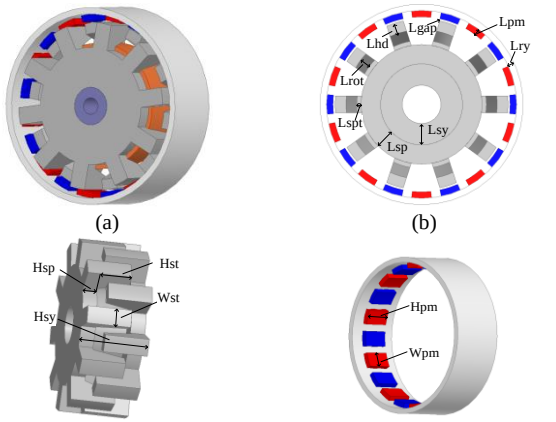

Fig. 1. 3-D design structure and parameters of the PM CPM with SMC cores

TABLE I
DESIGN OPTIMIZATION PARAMETERS AND RANGES

Par.	Description	Unit	Initial	Min	Max
W_{st}	tooth circumferential width	mm	8	7	10
W_{pm}	PM circumferential width	deg	12	10	14
H_{st}	Height of tooth	mm	14.35	10	16
B_r	PM remanence	T	1.15	1.10	1.30
L_{gap}	Length of air gap	mm	1.0	0.8	1.1
ρ	SMC core density	g/mm^3	7.32	6.75	7.35
N	Turns of coil	-	70	60	100

TABLE II
MEASURED AND CALCULATED PERFORMANCES OF PM CPM

Parameter	Unit	Calculated	Measured
Back EMF constant	V/rpm	0.0272	0.0271
No load core loss	W	58	60
Cogging torque peak	Nm	0.35	0.33
Coil temperature rise	°C	74	71

TABLE III
UNCERTAINTIES FOR THE DESIGN PARAMETERS

Par.	Unit	Uncertainties
W_{pm}	deg	Nominal ± 0.05
B_r	T	Nominal ± 0.05
L_{gap}	mm	Nominal ± 0.05
ρ	g/mm^3	Nominal ± 0.15
N	turns	Nominal ± 0.5

IV. COMPARISON OF MULTI-OBJECTIVE ROBUST DESIGN OPTIMIZATION METHODS

A. Applied Multi-objective Optimization Approaches

Based on the WC formulation of (2), the deterministic multi-objective optimization model of (5) can be converted into the following form.

$$\begin{aligned} \min:\ & \begin{cases} f_{w,1}(\mathbf{x}) = \max\limits_{\boldsymbol{\xi}\in U(\boldsymbol{\xi})} f_1(\mathbf{x},\boldsymbol{\xi}) \\ f_{w,2}(\mathbf{x}) = \max\limits_{\boldsymbol{\xi}\in U(\boldsymbol{\xi})} f_2(\mathbf{x},\boldsymbol{\xi}) \end{cases} \\ \text{s.t.}\ & g_{w,j}(\mathbf{x}) = \max_{\boldsymbol{\xi}\in U(\boldsymbol{\xi})} g_j(\mathbf{x},\boldsymbol{\xi}) \le 0, j = 1,2,\dots,5 \\ & U(\boldsymbol{\xi}) = \{\boldsymbol{\xi} \in R^5 | \Delta\boldsymbol{\xi} = [0.05, 0.05, 0.05, 0.15, 0.5]^T\} \end{aligned} \quad (6)$$

where optimization variables ($\mathbf{x}$) are the seven parameters listed in Table I.

Based on previous experience on the manufacturing of several SMC motors, there are no significant variations for the dimension of SMC tooth (the stator tooth) because the SMC stator is manufactured by using molding instead of the lamination technology. It is also a major advantage of SMC motors as this manufacturing method is good for mass production at low cost. Thus, no uncertainty information will be applied to the two parameters related to the SMC stator (W_{st} and H_{st}). Consequently, there are only five parameters in the uncertainty parameter vector $\boldsymbol{\xi}$. Experience is also applied to determine the variation of the air gap length and the winding turns. For the variations of other parameters, like the PM remanence and SMC core density, they are determined based on previous measurements [2,17]. Table III tabulates the uncertainties for these five design parameters. $\Delta\boldsymbol{\xi}$ in (6) represents the variation ranges of these parameters.

Similarly, the DFSS multi-objective optimization model of this SMC motor, based on (3) and (5), can be expressed as

$$\begin{aligned} \min:\ & \begin{cases} \mu[f_1(\mathbf{x})] \\ \mu[f_2(\mathbf{x})] \end{cases} \\ \text{s.t.}\ & \mu[g_j(\mathbf{x})] + 6\sigma[g_j(\mathbf{x})] \le 0, j = 1,2,\dots,5 \end{aligned} \quad (7)$$

B. Optimization Methods

For the optimization of models (5) to (7), a kind of multi-objective genetic algorithm, the non-dominated sorting genetic algorithm (NSGA) II, is used in this work [34]. The population size is 40. To conduct the optimization, there are two typical ways.

The first one is based on the multiphysics analysis models directly. This may require about 12,000 simulations (40×300, where 300 is a typical number for the number of generations used for NSGA II) of both 3-D FEM and 3-D thermal network model for the deterministic multi-objective optimization. For the robust multi-objective optimization, even significantly more simulations are required to evaluate the robustness of each design candidate (one of the 12,000 simulations in the deterministic approach). For example, extra 10,000 points are needed if MCA is used. To reduce the computation cost, several local approximate methods, like Taylor series, are used. If the first-order Taylor series is applied, 4 extra FEM samples are required for one design candidate [30,35]. Thus, 48,000 (12,000×4) FEMs are required. As a consequence, the total

required number of multiphysics simulations will be huge. This approach may work for some motors with simple 2-D FEM and a small number of design parameters, but it is not recommended for motors with 3-D FEM or many design parameters.

The second way is based on the approximate models or surrogate models, such as response surface model (RSM) and Kriging model [2]. In the implementation, RSM or Kriging model is developed first to approximate the multiphysics analysis models. Then, the optimization can be conducted based on the developed RSM or Kriging models. The main computation cost of this method is the samples for the modeling. For this motor, if a 5-level full-factor design is applied to the six parameters in the FEM, 15,625 (5^6) FEM simulations will be required for both deterministic and robust multi-objective optimization. This is acceptable for the robust design optimization of some motors with no time-consuming multiphysics analysis models. However, it is still too much for the investigated PM SMC motor as it requires several minutes for one simulation due to the calculation of both alternating and rotational core losses.

Based on previous research work and prototyping experience, four levels can be applied to several parameters, such as the air gap and core density. Five levels will be employed for other parameters. Thus, 6,400 FEMs are sampled to develop the approximate model for the optimization of (5)-(7). Regarding the approximate model, Kriging is employed in this work due to its superior modeling ability in both local and global region. It is a semi-parametric model and consists of a determined term like RSM and a random term. It has been claimed to be more accurate than RSM and has been widely employed in the optimization work of electromagnetic devices [36]. The detailed modeling process of Kriging model can be found in [37-39]. Please note that another step, verification of model accuracy, is required before starting the optimization based on some extra FEM samples. For the evaluation of model accuracy, several measures like root mean square error can be used. More details can be found in previous work [39].

C. Optimization Results and Discussions

Figure 2 shows the optimization results of the three multi-objective optimization methods, deterministic approach (illustrated as DA in Fig. 2a), WC robust approach and DFSS robust approach. As shown, for the same material cost, like AUD 15, the output power of the motor with optimal DA design is around 750 W, which is higher than that of WC (around 620 W) and DFSS (around 680 W). Therefore, the deterministic approach can provide the maximal output power while WC approach will have the minimum output power for a given material cost for the investigated SMC motor.

Figure 3 illustrates the PoF values of all Pareto optimal points for these three multi-objective optimization approaches. As shown, the PoF values of WC and DFSS designs are zero, which are much better than those of the deterministic approach. The minimal and maximal PoFs of the deterministic approach are 0.07% (the 6^{th} point) and 73.81% (the last point or 40^{th} point), respectively. The average PoF of all 40 points is 44.55%. Therefore, the higher output power given by the deterministic approach, as shown in Fig. 2, is obtained at the cost of high PoF, which is not acceptable in terms of batch/massive industrial production.

Figure 4 shows the sigma levels of all Pareto optimal points for these three multi-objective methods. As shown, all WC and DFSS Pareto optimal points can reach 6 sigma levels, while the maximal sigma level of deterministic approach is 3.39 (the 6^{th} point with PoF 0.07%), which is much smaller than 6. This figure illustrates a more clear comparison (a small difference of the PoF means a big difference in terms of sigma level) of the deterministic and robust multi-objective design optimization approaches. To have a further understanding of the higher PoF of the deterministic approach, Fig. 5 illustrates the PoF values of five constraints for all Pareto optimal points. As shown, the third and fourth constraint (slot filling factor and winding temperature rise) have high PoF values. Meanwhile, the first constraint also contributes to the cumulative PoF for the first five Pareto optimal points.

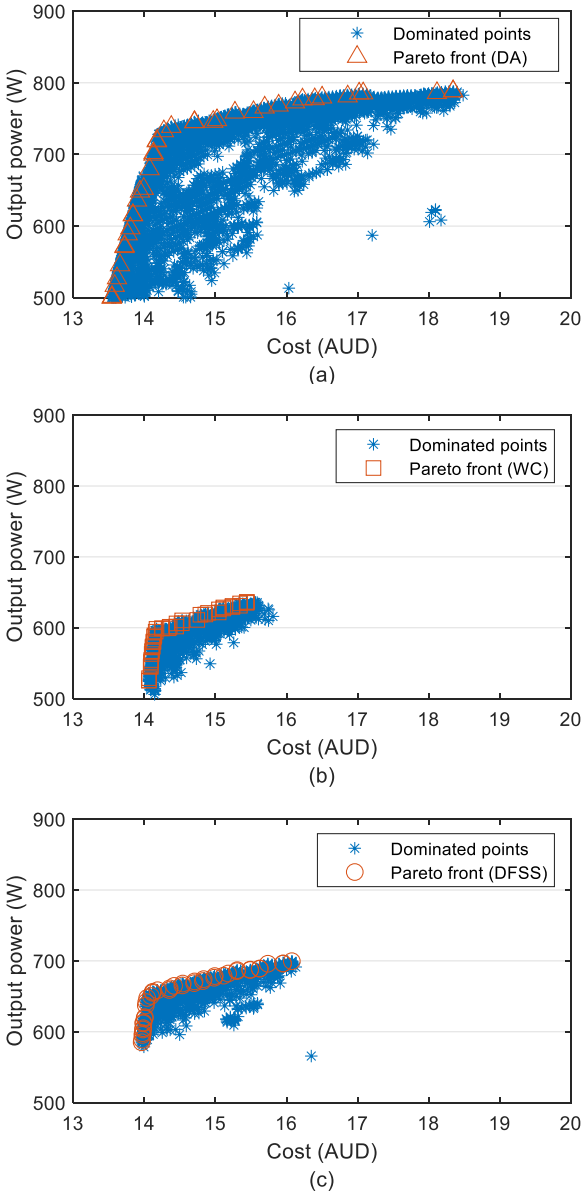

Fig. 2. Pareto fronts for three multi-objective optimization methods, (a) Deterministic, (b) WC, and (c) DFSS

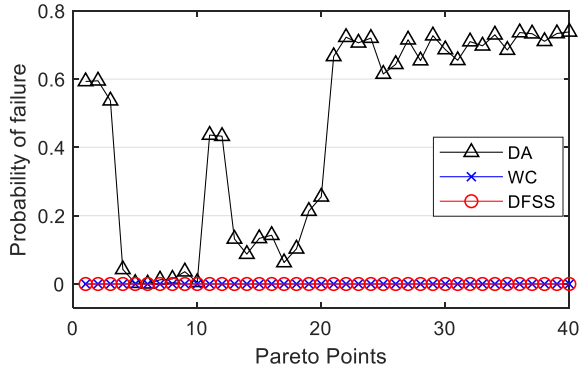

Fig. 3. PoF values of all Pareto optimal points for three multi-objective optimization methods

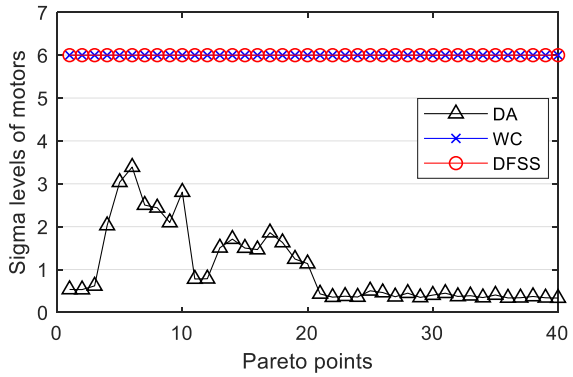

Fig. 4. Sigma levels of all Pareto optimal points for three multi-objective optimization methods

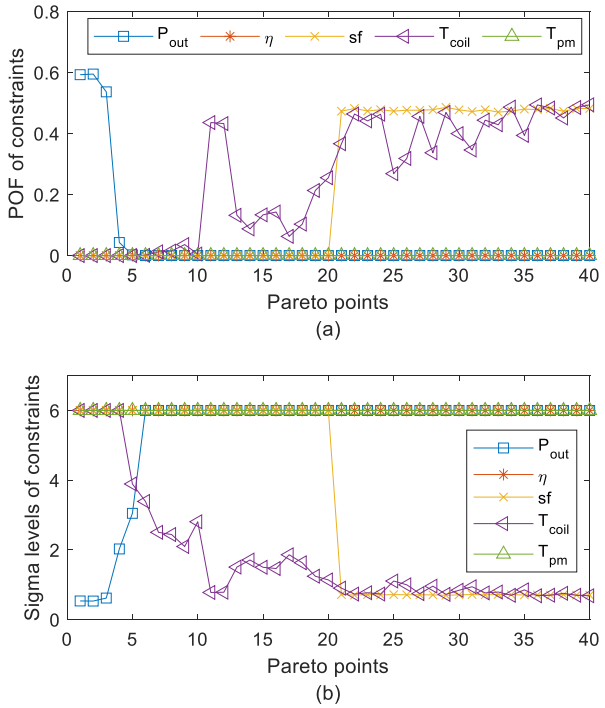

Fig. 5. PoF values and sigma levels of all Pareto optimal points of the deterministic approach, when applying the five considered constraints

TABLE IV
DESIGN PARAMETERS AND MOTOR PERFORMANCE OF THE LAST PARETO POINT FOR THREE MULTI-OBJECTIVE OPTIMIZATION METHODS

Par.	Unit	DA	WC	DFSS
L_{gap}	mm	1.09	0.80	1.00
W_{st}	mm	8.10	7.25	8.00
W_{pm}	deg	13.10	10.10	10.65
H_{st}	mm	11.60	10.25	10.75
B_r	mm	1.20	1.30	1.30
ρ	g/cm^3	6.75	6.85	6.80
N	turns	94	89	89
Cost	AUD	18.3	15.3	16.1
P_{out}	W	788	684	700
η	%	87.51	86.80	86.81
sf	-	0.70	0.66	0.66
T_{coil}	℃	75.0	70.1	70.7
T_{pm}	℃	58.5	53.8	54.9

As an example of a detailed comparison, Table IV lists the optimal parameters and motor performance of the last Pareto point (the one with the highest output power) for three multi-objective optimization methods. As can be seen, the deterministic approach provides the highest output power, however, the slot filling factor is 0.7 and the winding temperature rise is 75 ℃, which are exactly the same of the design limits. With the consideration of uncertainties, the practical motor performance in batch production, like the winding temperature rise, will violate the limit. This will result in a non-zero PoF for the motor. Figures 6-8 show the distributions of motor performance obtained from MCA for the last Pareto optimal point of three multi-objective optimization methods. As can be seen in Fig. 6e, around half of the simulation points are over the limit of temperature rise (75℃), which result in a big PoF for this constraint as well as for the motor. A similar situation applies to the third constraint. This confirms the analysis results shown in Fig. 5. For the WC and DFSS methods, as shown in Figs. 7 and 8, the values of all simulation points are away from the limits. For example, the maximal winding temperature rises are 74 ℃ for all simulation points in the MCA for both WC and DFSS methods.

The last comparison considers the deviation of the motors' performances. Figures 6-8 show the distributions of various motor performances for one Pareto optimal point after MCA. Mean and SD of each performance index, like the winding temperature rise, can be obtained for that point (the last Pareto point in this case). Similarly, the means and SDs of other Pareto optimal points (points 1-39) can be gained for each performance index. As an example, Fig. 9 shows the values of mean and SD of the winding temperature rise for all Pareto points for three multi-objective methods. As can be seen, the SD of WC and DFSS robust methods are less than those of the deterministic approach. To clearly show the advantage of the robust approaches, the average SDs of all five constraints are listed in Table V, including the winding temperature rise. As shown, the WC and DFSS have smaller average SDs, meaning smaller performance variation in the batch production. This is another advantage of robust design optimization method compared with deterministic design optimization.

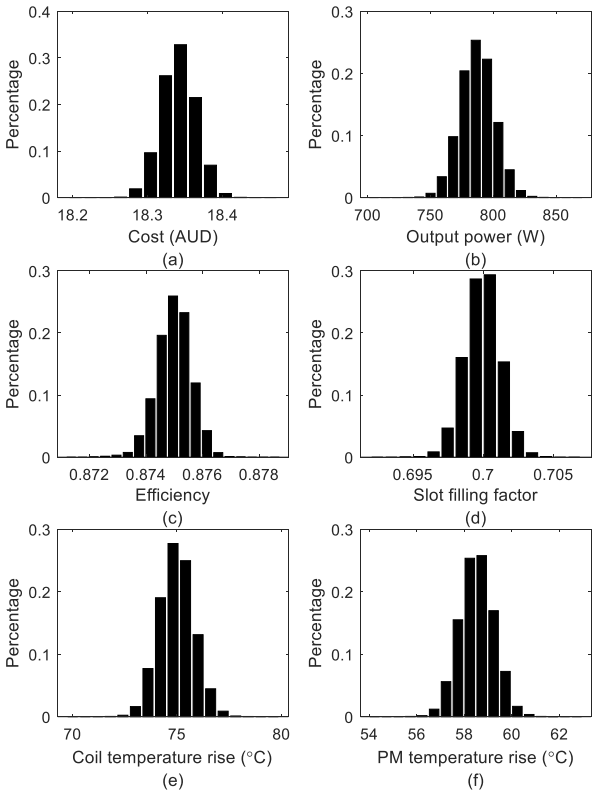

Fig. 6. Distribution of motor performance for the last Pareto optimal point (the one with the highest output power) of the deterministic approach

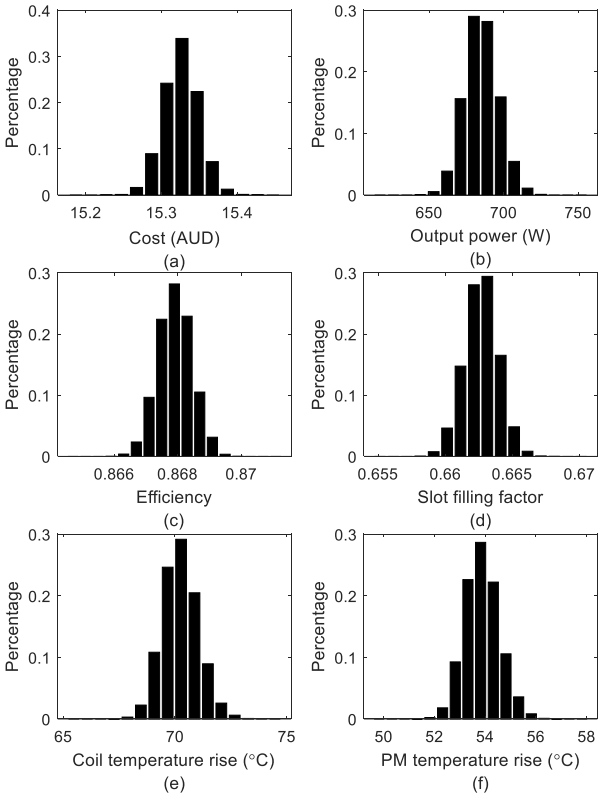

Fig. 7. Distribution of motor performance for the last Pareto optimal point (the one with the highest output power) of WC approach

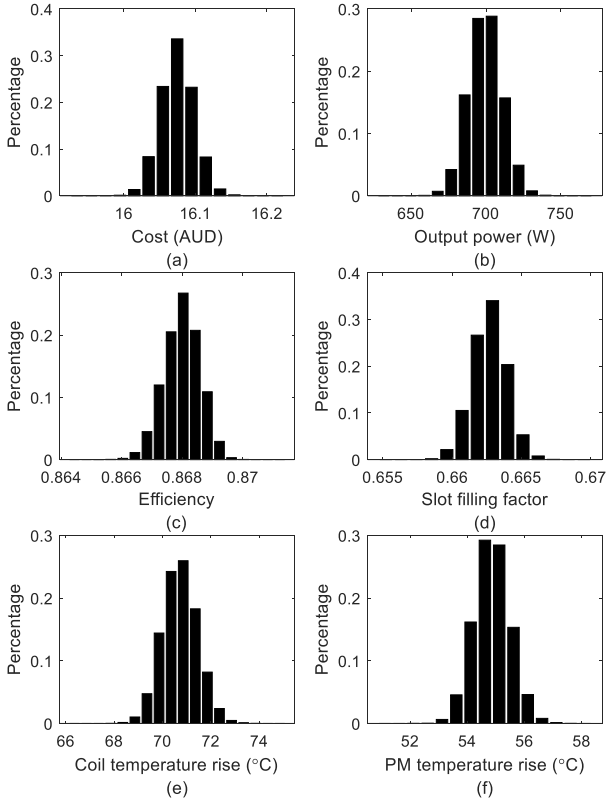

Fig. 8. Distribution of motor performance for the last Pareto optimal point (the one with the highest output power) of DFSS approach

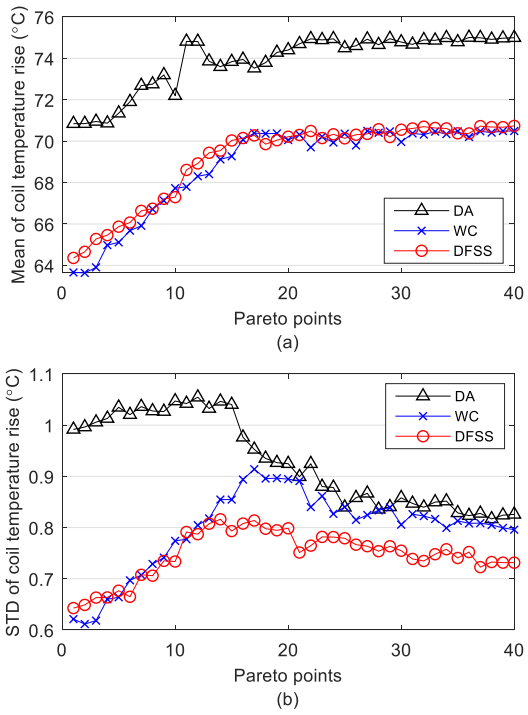

Fig. 9. Mean and SD of the coil temperature for all Pareto optimal points for three multi-objective optimization methods

TABLE V
AVERAGE SDS OF ALL CONSTRAINTS

	Unit	DA	WC	DFSS
P_{out}	W	11.90	11.15	10.95
η	%	0.08	0.06	0.07
sf	-	0.001	0.001	0.001
T_{coil}	℃	0.93	0.80	0.75
T_{pm}	℃	0.80	0.68	0.64

Through the case study and comparison, it is also found that DFSS is better than WC in several aspects. First, the derived optimal DFSS motor designs have a better performance, like higher output power for a given material cost. Second, no further optimization steps are required for DFSS, while WC is a minimax optimization problem (dual optimization is required) and will complicate the optimization process. This will also increase the computational burden of multi-objective robust optimization.

D. Comments on the Computation Cost

The computation cost of optimizing (5)-(7) consists of two main parts, the simulation time of FEM samples in *ANSYS* and the run time of optimization algorithm in *Matlab*.

The FEM simulation work is conducted in a cluster of our university. The main features of the used node are processor (Intel CPU 8 cores with base speed 2.9 GHz) and memory (32 GB RAM). As this is a 3-D FEM and both alternating and rotational core losses are needed to calculate, the average simulation time of each sample is 2 minutes. Thus, around 213 hours are required to simulate those 6,400 FEM samples for the development of Kriging model.

The optimization algorithm is run on a laptop. The main features of the used node are processor (Intel CPU 4 cores with base speed 1.9 GHz) and memory (8 GB RAM). The average running times of a deterministic and a robust (WC/ DFSS) optimization process are 20 minutes and 12 hours, respectively. Therefore, the FEM simulation time takes a major part of the total computation time. Consequently, in this work, we only compare the required FEM samples for different methods.

V. A NEW MSOM FOR HIGH-DIMENSIONAL MULTI-OBJECTIVE ROBUST OPTIMIZATION

Besides the multiphysics analysis models and uncertainty characterization, a major challenge of robust multi-objective optimization is the huge computation cost due to the large robustness evaluations. Though the approximate models (the second way mentioned in subsection IV-B) can be employed to alleviate this problem, it is still not applicable for many situations, like high-dimensional problems. Please note that there is not a definite value for the number of dimensions of high-dimensional problems, as it relates to the complexity and simulation time of the analysis models (like 2-D or 3-D FEMs) and the optimization model (like deterministic and robust optimization models).

In the field of design optimization of electromagnetic devices including electrical machines, if the performance of the device is based on the finite element analysis, the common practice of definition of a high-dimensional design problem is based on the number of the parameters. If the simulation time of an electrical machine design is more than 1 minute and the optimization parameters are no less than 6, this kind of problem can be regarded as a high-dimensional optimization problem. The main reason for this is that at least 4^6=4,096 samples (6 parameters with four levels for each parameter) will be required to develop the approximate model. If 5 levels are applied to each parameter, then 5^6=15,625 samples are required. The simulation process will be time-consuming. With the increase of one more parameter, the total number of required samples will be increased by 4 or 5 times if 4 or 5 levels are assigned for that parameter. Therefore, it is very hard to use conventional robust multi-objective optimization methods to solve these high-dimensional optimization problems. To attempt this challenge, a new and efficient multi-objective robust optimization method is proposed in this section.

Figure 10 shows the flowchart of the proposed new MSOM. The main idea of this method is to update the Pareto front by improving the approximate models with less samples sequentially. The method includes five main steps.

Step 1: Define the multi-objective robust optimization problems, including objective functions, constraints, design parameters and their ranges, uncertainty parameters and information, for the investigated electrical machine. Meanwhile, develop the analysis models for the performance evaluation of electrical machines, such as the FEM for magnetic field analysis, the thermal network model for the analysis of temperature rise, and the FEM for the stress and modal analysis.

Step 2: Generate samples, simulate their responses and develop approximate models based on the samples. As it is hard to use high levels for all factors for high-dimensional situation and the Pareto front is expected to be improved step by step, a three-level full-factorial design is recommended in this step. The required simulation samples will be reduced greatly. For example, only 3^6=729 samples are required for a multi-objective optimization problem with six parameters in the FEM. For a problem with eight parameters, 3^8=6,561 samples are necessary. This is acceptable if the FEM is not very time-consuming. The initial set of samples is defined as S(1).

To develop the approximate models based on S(1), a type of approximate model should be chosen first, for example, a RSM with a quadratic polynomial. Then, the data S(1) will be used to estimate the coefficients of the quadratic polynomial based on several parameter estimation methods in Statistics, like the least square method. For a Kriging model, as it includes a random term, maximum likelihood estimation may be required as well. More details of the development of approximate models can be found in [39].

Step 3: Conduct the multi-objective optimization based on beforehand developed approximate models and NSGA II. A Pareto optimal front with a certain number of points can be obtained. For these points, calculate their hypervolume indicator (I_h) with respect to a reference point. Fig. 11 illustrates an example of the calculation of the hypervolume indicator for a two objective situation with five Pareto points. In this case, the hypervolume indicator is actually the area of the shaded part [40,41]. The main reason for using the hypervolume indicator is that it can evaluate the convergence behavior and uniformity of the Pareto solutions at the same time [42,43].

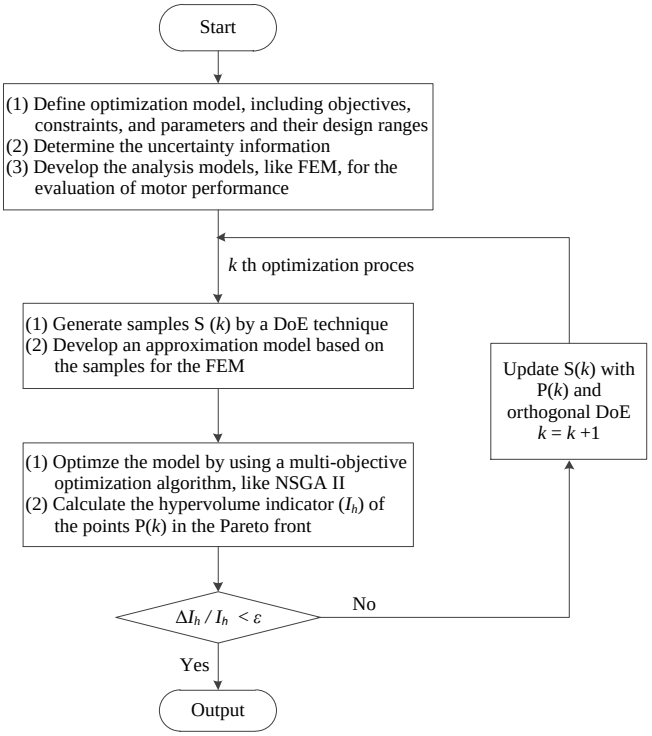

Fig. 10. Flowchart of the proposed new MOSM

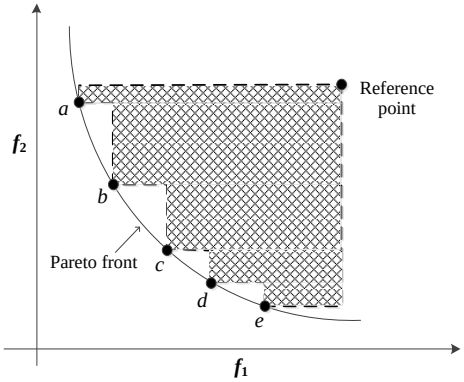

Fig. 11. Illustration of the hypervolume indicator for two objectives situation

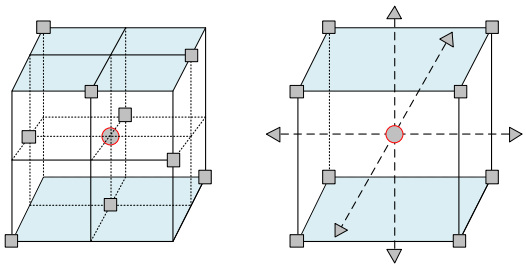

Fig. 12. (a) An orthogonal design sampling, and (b) a modified CCD sampling

Step 4: Compare the hypervolume indicator of two continuous iterations of this MSOM. If the relative change between two iterations is smaller than a specific value ε (like 5% or 2.5%), finish the optimization process and output the obtained Pareto optimal designs and front. Otherwise, go to the next step, update the samples and approximate models, and re-implement the multi-objective optimization process until the convergence criterion is met.

Step 5: Update the samples and approximate models by using an orthogonal design technique. If the analysis models are accurate, the obtained Pareto optimal front should be located in a small area of the final Pareto front. The next step is to update the points in the front. For this purpose, new samples are required to update the approximate models.

If a three-level full-factor design is employed, there will be 3^6=729 new samples for each point in the Pareto front, resulting in 29,160 (729×40) new samples, which is huge and not implementable. To overcome this issue, orthogonal design is suggested here. In statistics, orthogonal design is more efficient (fewer samples) than the full-factorial design for the data analysis like analysis of variance.

Figure 12 shows the samples for an orthogonal design with three levels for three design parameters. As shown, only nine samples (indicated as squares) are required, which is less than the 27 samples (vertex and intersections of lines) required by a full-factorial design. This orthogonal design can be applied to up to four design parameters and the corresponding orthogonal array is normally termed as $L^9(3^4)$, as listed in Table VI. As shown, the first column represents the number of experiment (equivalent to one FEM simulation), from 1 to 9; the first row stands for the number of parameters, from 1 to 4. As there are only 3 parameters in Fig. 12, we may just use the columns 2-4 to define the 9 samples (covered by the double-line boundary), where 1, 2, and 3 give the selected level of a parameter (for example, 0.8, 0.9, and 1.0 mm for the length of the air gap).

TABLE VI
AN EXAMPLE OF ORTHOGONAL ARRAY $L_9(3^4)$

No. of exp.	Parameters			
	1	**2**	**3**	**4**
1	1	1	3	2
2	2	1	1	1
3	3	1	2	3
4	1	2	2	1
5	2	2	3	3
6	3	2	1	2
7	1	3	1	3
8	2	3	2	2
9	3	3	3	1

As we have 6 parameters in the FEM of this motor, an orthogonal design $L_{27}(3^{13})$ is recommended for the proposed MSOM. It can handle up to 13 design parameters and only 27 points are required for each point in the Pareto front. Thus, only 1,080 (27×40) new samples are needed for updating of the samples and models in each iteration of MSOM. In the implementation, the step size of two levels is initially defined as the step size of the corresponding parameter in the S(1), then it will be halved in the next iteration as the Pareto front should be more and more accurate with the updating process.

Furthermore, to ensure the accuracy of the approximate model, there should be enough distance for any two points, otherwise, the inversion of matrix will be ill-posed. This can further reduce the new samples and increase the optimization efficiency as well.

Compared with the previous MSOM mentioned in [44,45], the new MSOM has two main differences. First, a modified central composite design (CCD) was used in previous work; however, it is not suitable for this high-dimensional case. For example, Fig. 12b shows the new samples for a three parameters case. As shown, 14 samples (six triangles and 8 squares) are required. In general, $2D+2^D$ new samples are required for an optimization problem with D parameters. Thus, 76 new samples are needed for the optimization of the investigated motor. Consequentially, 3040 (76×40) new samples are required for each iteration of MSOM, which is significantly larger than those of orthogonal design. Second, root mean square error is used as the convergence criterion, which is not based on the comparison of the Pareto fronts. The hypervolume is better and more clear in terms of the theory of multi-objective optimization.

VI. Example Study for the New MSOM

This section illustrates the performance of the proposed MSOM by using two design approaches, deterministic and DFSS. As the performance of DFSS is better than WC, only DFSS will be investigated in this section. The value of ε in the proposed MSOM is set at 2.5%.

A. Deterministic Multi-objective Optimization

Figure 13 shows the Pareto optimal results of the MSOM for the deterministic multi-objective optimization of this motor by using model (5). As shown, four iteration processes, MSOM1, MSOM2, MSOM3, and MSOM4, are needed for the new MSOM. The hypervolume indicator of each iteration of new MSOM is shown in Fig. 14. For the calculation of the hypervolume indicator, the reference point is [19, 500]. As can be seen, the relative error of the hypervolume indicators of the last two iterations is 2.22%, which is smaller than the default value, 2.5%. As shown in Fig. 13, the Pareto fronts of the last two iterations are in good agreement. The first Pareto front, indicated as MSOM1, is not good, and there is an obvious difference between it and the one given by the conventional deterministic approach (indicated as DA in the figure). Then, a clear approaching process is observed for the following three Pareto fronts (from MSOM2 to MSOM4). Most importantly, the last Pareto optimal front given by the proposed new MSOM is better than that (red triangles in the figure) given by conventional deterministic approach.

To show more details of the obtained Pareto solutions, Table VII lists the parameter values and the corresponding motor performance of the last point in the Pareto front. As shown, the output power of the design variant obtained by the deterministic approach is 790 W. After Monte Carlo analysis, the PoF of this design is 0.74 (or 74%), which is very high.

For the computation cost of FEM, 6,400 FEMs are used for the conventional deterministic approach, which was discussed in section IV. For the new MSOM, 729, 720, 818 and 982 (3,249 in total) new samples are required for the four iterations, which is 50.8% of the one required by the conventional method. Therefore, the proposed method is efficient for deterministic multi-objective optimization.

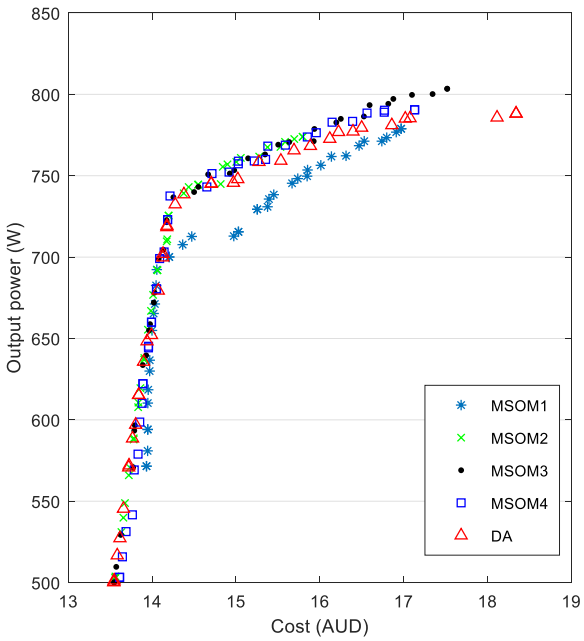

Fig. 13. Iteration process of the Pareto fronts for the deterministic multi-objective optimization by using the new MSOM

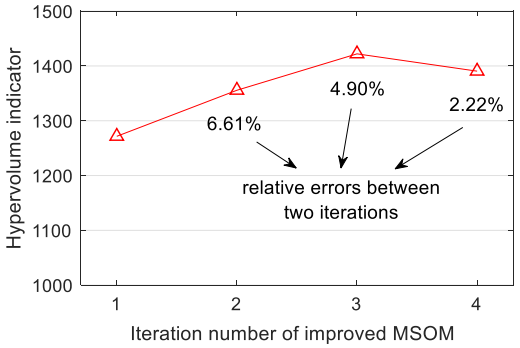

Fig. 14. The hypervolume indicator of the Pareto fronts for deterministic multi-objective optimization by using the new MSOM

TABLE VII
Design Parameters and Motor Performance of the Last Pareto Point for Designs Obtained from the New MSOM

Par.	Unit	DA-MSOM	DFSS-MSOM
L_{gap}	mm	0.81	0.91
W_{st}	mm	7.85	7.95
W_{pm}	deg	12.45	11.75
H_{st}	mm	10.65	1020
B_r	mm	1.15	1.20
ρ	g/cm^3	6.90	6.75
N	turns	94	93
$Cost$	AUD	17.1	16.7
P_{out}	W	790	723
η	%	87.64	87.31
sf	-	0.70	0.69
T_{coil}	℃	75.0	70.8
T_{pm}	℃	58.2	54.6
PoF	-	0.74	0

Last, a comment goes to the Pareto fronts of MSOM3 and MSOM4. As shown in Fig. 13, MSOM3 presents higher values of output power than MSOM4 for some points in the Pareto front. However, the difference between them is not significant. There are two possible reasons for the difference: First, the Kriging models for MSOM3 and MSOM4 optimization are slightly different, as some new points have been added to MSOM4. Second, there are some minor variations for the Pareto fronts due to the nature of multi-objective optimization algorithm and nonlinear optimization problems featuring a random component.

B. Robust Multi-objective Optimization based on DFSS

Figure 15 shows the Pareto optimal results of the MSOM for the DFSS multi-objective optimization of this motor by using model (7). As shown, five iteration processes are required for the proposed new MSOM. The hypervolume indicator of each iteration of new MSOM is shown in Fig. 16. For the calculation of the hypervolume indicator, the reference point is [17, 550]. As shown, the relative error of the hypervolume indicators of the last two iterations is 2.15%, which is smaller than the default value. As can be seen from Fig. 15, the Pareto fronts of the last two iterations are in good agreement. Most importantly, the last Pareto optimal front given by the proposed new MSOM is better than that of the conventional DFSS obtained in section IV. The parameter values and the corresponding motor performance of the last point in the Pareto front are listed in Table VII. As shown, the output power of the considered design variant is 723 W, which is slightly better than that of the conventional DFSS approach (700 W as listed in Table IV). After Monte Carlo analysis, the PoF this design is 0, meaning that six-sigma quality will be achieved in the manufacturing of this motor.

For the computation cost of FEM, 729, 687, 667, 788 and 765 (3,636 in total) new samples are required for the five iterations of the MSOM. This is 56.8% compared with the samples required by the conventional DFSS method. Therefore, the proposed method is efficient for the robust multi-objective optimization. Moreover, the final Pareto optimal front obtained from the MSOM is better than that of the conventional DFSS. The main reason for this fact is that the proposed multi-objective problem is a high-dimensional multiphysics problem. It has many local optimums. The results of the conventional methods may be better if there are more samples in the modelling process, but this will increase the computation burden.

C. Remarks on the New MSOM

First, please note that the obtained Pareto fronts and iterations of the proposed MSOM are related to the value ε. If 5% is selected as a measure, only two iterations are required for the deterministic multi-objective optimization. As shown in Fig. 14, the second relative error of the hypervolume indicator is 4.9%. As can be seen in Fig. 13, the obtained Pareto front (indicated as green x) is good as well, very close to the DA. For the DFSS, only one MSOM is required. Similarly, the obtained Pareto front (indicated as green x) is acceptable as well.

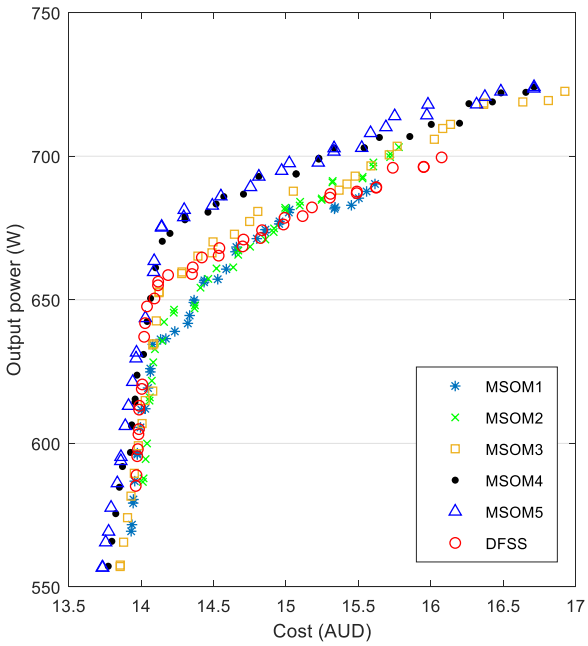

Fig. 15. Iteration process of the Pareto fronts for the DFSS multi-objective optimization by using the new MSOM

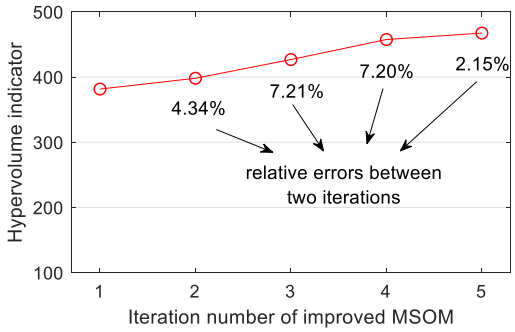

Fig. 16. The hypervolume indicator of the iteration process of the Pareto fronts of DFSS multi-objective optimization

Second, the proposed MSOM can be applied to an optimization problem with up to eight design parameters for analyses based on FEM. In addition, several other parameters that do not require FEM analyses can additionally be added, like winding parameters (number of turns and winding diameter). Therefore, around 10 parameters can be effectively handled by this method. Consequently, most high-dimensional robust multi-objective optimization problems of electrical machines can be solved by utilizing this method.

Third, the proposed method can be applied to a design problem with more than three objectives. However, the calculation of the hypervolume indicator will be harder with the increasing number of objectives. Fortunately, some research works have investigated this problem theoretically (many-objective situation) in the field of evolutionary computation. There are several methods to handle this problem [41-43]. Therefore, this should not be a big problem for the application of this method to most multi-objective problems of electrical machines.

Fourth, to further increase the optimization efficiency, parallel computation and pre-robustness analysis can be applied. For the pre-robustness analysis, it means to determine

which designs in the population are required to conduct the robustness analysis. If a design does not satisfy the constraints for rated parameters, robust analysis is not required at all, and this can save a lot of computation cost for the overall optimization.

Last, this paper focuses on the development of a generic multi-objective optimization method. It should be meaningful and promising to apply it to motors used in some specific applications, especially for those applications of new/advanced magnetic materials for drive/propulsion systems, such as the linear propulsion systems with superconducting motors for maglevs [46-48] and the motors with amorphous cores for electric vehicles [49,50]. There should be more opportunities in these topics with the investigation of different manufacturing methods and uncertainty information for the new/advanced materials.

VII. Conclusion

This paper presented a comparative study for three popular multi-objective design optimization methods for electrical machines, including two robust approaches based on WC and DFSS designs. To efficiently attempt high-dimensional multi-objective robust optimization problems, a new MSOM with an orthogonal design technique and hypervolume indicator was proposed. A design example was investigated to compare the performance of different multi-objective optimization methods. Through the comparison, the following conclusions can be drawn.

First, regarding the deterministic and robust multi-objective optimization, it is found that the two robust approaches are better than the deterministic approach from a reliability point of view, as the PoF of the robust methods can be decreased to zero. Moreover, the averaged SDs of the motors' performances obtained by the robust methods are smaller than that of the deterministic approach, meaning smaller quality variation in production. Moreover, DFSS is better than WC in terms of motor performance and computation cost.

Second, the proposed new MSOM is efficient for the high-dimensional deterministic and robust multi-objective optimization of electrical machines. Through the case study, the FEM samples required by the new MSOM are less than 60% of those required by the conventional methods, while the obtained motor performance is better. Furthermore, several remarks are presented for the application of the proposed method.

References

[1] G. Bramerdorfer, J. A. Tapia, J. J. Pyrhönen and A. Cavagnino, "Modern electrical machine design optimization: techniques, trends, and best practices," *IEEE Trans. Ind. Electron*., vol. 65, no. 10, pp. 7672-7684, Oct. 2018.

[2] G. Lei, J. Zhu, Y. Guo, C. Liu and B. Ma, "A review of design optimization methods for electrical machines", *Energies*, vol. 10, no. 12, Art. no. 1962, pp. 1-31, Dec. 2017.

[3] G. Du, W. Xu, J. Zhu and N. Huang, "Rotor Stress Analysis for High-Speed Permanent Magnet Machines Considering Assembly Gap and Temperature Gradient," *IEEE Trans. Energy Convers*., vol. 34, no. 4, pp. 2276-2285, Dec. 2019.

[4] T. de Paula Machado Bazzo, J. F. Kölzer, R. Carlson, F. Wurtz and L. Gerbaud, "Multiphysics Design Optimization of a Permanent Magnet Synchronous Generator," *IEEE Trans. Ind. Electron*., vol. 64, no. 12, pp. 9815-9823, Dec. 2017.

[5] Z. Stephen Du, J. Tangudu, A. Sur and S. Soni, "Multiphysics Design and Optimization for a SPM Machine with MnBi Magnet and 6.5% Silicon Steel Materials for Traction Applications," 2019 IEEE International Electric Machines & Drives Conference (IEMDC), San Diego, CA, USA, 2019, pp. 1001-1008.

[6] Z. Huang and J. Fang, "Multiphysics Design and Optimization of High-Speed Permanent-Magnet Electrical Machines for Air Blower Applications," *IEEE Trans. Ind. Electron*., vol. 63, no. 5, pp. 2766-2774, May 2016.

[7] D. Yao and D. M. Ionel, "A review of recent developments in electrical machine design optimization methods with a permanent magnet synchronous motor benchmark study", *IEEE Trans. Industry Appl*., vol. 49, no. 3, pp. 1268-1275, Sep. 2013.

[8] J. Song, F. Dong, J. Zhao, H. Wang, Z. He and L. Wang, "An Efficient Multiobjective Design Optimization Method for a PMSLM Based on an Extreme Learning Machine," *IEEE Trans. Ind. Electron*., vol. 66, no. 2, pp. 1001-1011, Feb. 2019.

[9] E. Howard and M. J. Kamper, "Weighted Factor Multiobjective Design Optimization of a Reluctance Synchronous Machine," *IEEE Trans. Industry Appl*., vol. 52, no. 3, pp. 2269-2279, May-June 2016.

[10] X. Zhu, D. Fan, L. Mo, Y. Chen and L. Quan, "Multiobjective Optimization Design of a Double-Rotor Flux-Switching Permanent Magnet Machine Considering Multimode Operation," *IEEE Trans. Ind. Electron*.,vol. 66, no. 1, pp. 641-653, Jan. 2019.

[11] X. Jannot, J. Vannier, C. Marchand, M. Gabsi, J. Saint-Michel and D. Sadarnac, "Multiphysic Modeling of a High-Speed Interior Permanent-Magnet Synchronous Machine for a Multiobjective Optimal Design," in *IEEE Trans. Energy Convers*., vol. 26, no. 2, pp. 457-467, June 2011.

[12] D. Lim, D. Woo, H. Yeo, S. Jung, J. Ro and H. Jung, "A Novel Surrogate-Assisted Multi-Objective Optimization Algorithm for an Electromagnetic Machine Design," *IEEE Trans. Magn.*, vol. 51, no. 3, pp. 1-4, March 2015, Art no. 8200804.

[13] X. Zhu, W. Wu, L. Quan, Z. Xiang and W. Gu, "Design and multi-objective stratified optimization of a less-rare-earth hybrid permanent magnets motor with high torque density and low cost," *IEEE Trans. Energy Convers*., vol. 34, no. 3, pp. 1178-1189, Sept. 2019.

[14] Y. Mao, S. Niu and Y. Yang, "Differential Evolution-Based Multiobjective Optimization of the Electrical Continuously Variable Transmission System," *IEEE Trans. Ind. Electron*., vol. 65, no. 3, pp. 2080-2089, March 2018.

[15] Y. Ma, T. W. Ching, W. N. Fu and S. Niu, "Multi-Objective Optimization of a Direct-Drive Dual-Structure Permanent Magnet Machine," *IEEE Trans. Magn.*, vol. 55, no. 10, pp. 1-4, Oct. 2019, Art no. 7501704.

[16] G. Lei, T. Wang, J. Zhu, Y. Guo, and S. Wang, "System-level design optimization method for electrical drive systems-robust approach," *IEEE Trans. Ind. Electron.*, vol. 62, no. 8, pp. 4702-4713, 2015.

[17] B. Ma, G. Lei, J. G. Zhu, Y. G. Guo and C. C. Liu, "Application-oriented robust design optimization method for batch production of permanent-magnet motors," *IEEE Trans. Ind. Electron*., vol. 65, no. 2, pp. 1728-1739, 2018.

[18] F. Dong, J. Song, J. Zhao and J. Zhao, "Multi-objective design optimization for PMSLM by FITM," *IET Electr. Power Appl.*, vol. 12, no. 2, pp. 188-194, 2018.

[19] S. Lee, K. Kim, S. Cho, J. Jang, T. Lee and J. Hong, "Optimal design of interior permanent magnet synchronous motor considering the manufacturing tolerances using Taguchi robust design," *IET Electr. Power Appl.*, vol. 8, no. 1, pp. 23-28, January 2014.

[20] K. S. Kim, K. T. Jung, J. M. Kim, J. P. Hong and S. I. Kim, "Taguchi robust optimum design for reducing the cogging torque of EPS motors considering magnetic unbalance caused by manufacturing tolerances of PM," *IET Electr. Power Appl.*, vol. 10, no. 9, pp. 909-915, 11 2016.

[21] Z. Ren, M. Pham and C. S. Koh, "Robust global optimization of electromagnetic devices with uncertain design parameters: comparison of the worst case optimization methods and multiobjective optimization approach using gradient index," *IEEE Trans. Magn.*, vol. 49, no. 2, pp. 851-859, Feb. 2013.

[22] Z. Ren, D. Zhang and C. Koh, "New reliability-based robust design optimization algorithms for electromagnetic devices utilizing worst case scenario approximation," *IEEE Trans. Magn.*, vol. 49, no. 5, pp. 2137-2140, May 2013.

[23] S. Xiao, Y. Li, M. Rotaru and J. K. Sykulski, "Six Sigma Quality Approach to Robust Optimization," *IEEE Trans. Magn.*, vol. 51, no. 3, pp. 1-4, March 2015, Art no. 7201304.

[24] M. A. Khan, I. Husain, M. R. Islam, and J. T. Klass, "Design of experiments to address manufacturing tolerances and process variations

influencing cogging torque and back EMF in the mass production of the PMSMs," *IEEE Trans. Ind. Appl.*, vol. 50, no. 1, pp. 346-355, 2014.
[25] A. J. Pina and L. Xu, "Analytical prediction of torque ripple in surface-mounted permanent magnet motors due to manufacturing variations," *IEEE Trans. Energy Convers.*, vol. 31, pp. 1634-1644, 2016.
[26] G. Bramerdorfer, "Tolerance Analysis for Electric Machine Design Optimization: Classification, Modeling and Evaluation, and Example," *IEEE Trans. Magn.*, vol. 55, no. 8, pp. 1-9, Aug. 2019, Art no. 8106809.
[27] G. Bramerdorfer and A. Zăvoianu, "Surrogate-Based Multi-Objective Optimization of Electrical Machine Designs Facilitating Tolerance Analysis," *IEEE Trans. Magn.*, vol. 53, no. 8, pp. 1-11, Aug. 2017.
[28] X. Ge and Z. Q. Zhu, "Influence of manufacturing tolerances on cogging torque in interior permanent magnet machines with eccentric and sinusoidal rotor contours," *IEEE Trans Ind. Appl*., vol. 53, no. 4, pp. 3568-3578, July-Aug. 2017.
[29] I. Coenen, M. Giet, and K. Hameyer, "Manufacturing tolerances: Estimation and prediction of cogging torque influenced by magnetization faults," *IEEE Trans. Magn.*, vol. 48, no. 5, pp. 1932-36, May 2012.
[30] P. N. Koch, R. J. Yang, and L. Gu. "Design for six sigma through robust optimization," *Struct. Multidiscip. Optim.*, vol. 26, no. 3-4, pp. 235-248, 2004.
[31] C. Liu, G. Lei, T. Wang, Y. Guo, Y. Wang, and J. Zhu, "Comparative study of small electrical machines with soft magnetic composite cores," *IEEE Trans. Ind. Electron.*, vol. 64, no. 2, pp. 1049-1060, 2017.
[32] J. G. Zhu, Y. G. Guo, Z. W. Lin, Y. J. Li, and Y. K. Huang, "Development of PM transverse flux motors with soft magnetic composite cores," *IEEE Trans. Magn*., vol. 47, no. 10, pp. 4376-4383, Oct. 2011.
[33] B. Ma, G. Lei, J. Zhu and Y. Guo, "Design optimization of a permanent magnet claw Pole motor with soft magnetic composite cores," *IEEE Trans. Magn.*, vol. 54, no. 3, pp. 1-4, March 2018, Art no. 8102204.
[34] K. Deb, A. Pratap, S. Agarwal, and T. Meyarivan, "A fast and elitist multi-objective genetic algorithm: NSGA-II," *IEEE Trans. Evol. Comput*., vol. 6, no. 2, pp. 182–197, Apr. 2002.
[35] G. Lei, T. Wang, J. Zhu and Y. Guo, "Robust multiobjective and multidisciplinary design optimization of electrical drive systems," *CES Transactions on Electrical Machines and Systems*, vol. 2, no. 4, pp. 409-416, Dec. 2018.
[36] L. D. Wang and D. A Lowther, "Selection of approximation models for electromagnetic device optimization," *IEEE Trans. Magn*., vol. 42, no. 2, pp. 1227-1230, Feb. 2006.
[37] S. N. Lophaven, H. B. Nielsen, and J. Sondergaard, "DACE: A MATLAB Kriging toolbox version 2.0," Technical Report IMM-TR-2002-12, Technical University of Denmark, Copenhagen, 2002.
[38] G. Lei, T. Wang, J. Zhu, et al., "System level design optimization method for electrical drive systems: deterministic approach," *IEEE Trans. Ind. Electron*., vol. 61, no. 12, pp. 6591-6602, 2014.
[39] G. Lei, J. G. Zhu, and Y. G. Guo, *Multidisciplinary Design Optimization Methods for Electrical Machines and Drive Systems*, Springer, ISBN: 978-3-662-49269-7, 2016.
[40] S. Jiang, J. Zhang, Y. Ong, A. N. Zhang and P. S. Tan, "A Simple and Fast Hypervolume Indicator-Based Multiobjective Evolutionary Algorithm," *IEEE Transactions on Cybernetics*, vol. 45, no. 10, pp. 2202-2213, Oct. 2015
[41] A. P. Guerreiro and C. M. Fonseca, "Computing and Updating Hypervolume Contributions in Up to Four Dimensions," *IEEE Transactions on Evolutionary Computation*, vol. 22, no. 3, pp. 449-463, June 2018.
[42] A. Zăvoianu, E. Lughofer, G. Bramerdorfer, W. Amrhein, and E. P. Klement, "DECMO2: a robust hybrid and adaptive multi-objective evolutionary algorithm," *Soft Comput*, vol. 19, pp. 3551–3569, 2015.
[43] K. Shang, H. Ishibuchi and X. Ni, "R2-Based Hypervolume Contribution Approximation," *IEEE Transactions on Evolutionary Computation*, vol. 24, no. 1, pp. 185-192, Feb. 2020.
[44] G. Lei, X. M. Chen, J. G. Zhu, Y. G. Guo, W. Xu and K. R. Shao, "Multiobjective Sequential Optimization Method for the Design of Industrial Electromagnetic Devices," *IEEE Trans. Magn*., vol. 48, no. 11, pp. 4538-4541, Nov. 2012.
[45] G. Lei, J. Zhu, Y. Guo, K. Shao and W. Xu, "Multiobjective Sequential Design Optimization of PM-SMC Motors for Six Sigma Quality Manufacturing," *IEEE Trans. Magn*., vol. 50, no. 2, pp. 717-720, Feb. 2014, Art no. 7017704.
[46] F. Dong, Z. Huang, D. Qiu, L. Hao, W. Wu and Z. Jin, "Design and Analysis of a Small-Scale Linear Propulsion System for Mag-lev Applications (1)-The Overall Design Process," *IEEE Tran. Appl. Supercond.*, vol. 29, no.2, pp. 1-5, 2019, Art no. 5201005.
[47] F. Dong, Z. Huang, D. Qiu, L. Hao, W. Wu and Z. Jin, "Design and Analysis of a Small-Scale Linear Propulsion System for Maglev Applications (2)–The HTS No-Insulation Magnets," *IEEE Tran. Appl. Supercond.*, vol. 29, no. 2, pp. 1-5, 2019, Art no. 5200905.
[48] R. A. H. de Oliveira, R. M. Stephan and A. C. Ferreira, "Optimized Linear Motor for Urban Superconducting Magnetic Levitation Vehicles," *IEEE Trans. Appl. Supercond.*, vol. 30, no. 5, pp. 1-8, Aug. 2020, Art no. 3601808.
[49] J. Ou, Y. Liu, P. Breining, M. Schiefer and M. Doppelbauer, "Experimental Study of the Amorphous Magnetic Material for High-Speed Sleeve-Free PM Rotor Application," *IEEE Trans. Ind. Electron*., vol. 67, no. 6, pp. 4422-4432, June 2020.
[50] T. Li, Y. Zhang, Y. Liang, Q. Ai and H. Dou, "Multiphysics Analysis of an Axial-Flux In-Wheel Motor With an Amorphous Alloy Stator," *IEEE Access*, vol. 8, pp. 27414-27425, 2020.

Gang Lei (M'14) received the B.S. degree in Mathematics from Huanggang Normal University, China, in 2003, the M.S. degree in Mathematics and Ph.D. degree in Electrical Engineering from Huazhong University of Science and Technology, China, in 2006 and 2009, respectively.

He is currently a Senior Lecturer at the School of Electrical and Data Engineering, University of Technology Sydney (UTS), Australia. His research interests include computational electromagnetics, design optimization and control of electrical drive systems and renewable energy systems. He is an Associate Editor of the IEEE TRANSACTIONS ON INDUSTRIAL ELECTRONICS.

Gerd Bramerdorfer (S'10-M'14-SM'18) received the Ph.D. degree in electrical engineering from Johannes Kepler University Linz, Linz, Austria, in 2014. He is currently an Assistant Professor with the Department of Electrical Drives and Power Electronics, Johannes Kepler University Linz. His research interests include the design, modeling, and optimization of electric machines as well as magnetic bearings and bearingless machines.

Dr. Bramerdorfer is a Senior Member of IEEE, an Editor of the IEEE TRANSACTIONS ON ENERGY CONVERSION and a past Associate Editor of the IEEE TRANSACTIONS ON INDUSTRIAL ELECTRONICS.

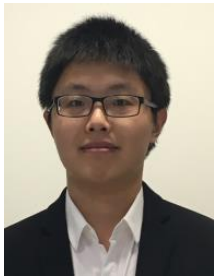

Bo Ma (M'15) Bo Ma received the B.E. degree in electrical engineering from Hefei University of Technology, Hefei, China, in 2014. He is currently working toward the Ph.D. degree in the School of Electrical and Data Engineering, University of Technology Sydney (UTS), Sydney, Australia.

His current research interests include design optimization of electrical machines and drive systems.

Youguang Guo (S'02-M'05-SM'06) received the B.E. degree from Huazhong University of Science and Technology, China in 1985, the M.E. degree from Zhejiang University, China in 1988, and the Ph.D. degree from University of Technology, Sydney (UTS), Australia in 2004, all in electrical engineering.

He is currently a Professor at the School of Electrical and Data Engineering, University of Technology Sydney (UTS). His research fields include measurement and modeling of properties of magnetic materials, numerical analysis of electromagnetic field, electrical machine design optimization, power electronic drives and control.

Jianguo Zhu (S'93–M'96–SM'03) received the B.E. degree in 1982 from Jiangsu Institute of Technology, Jiangsu, China, the M.E. degree in 1987 from Shanghai University of Technology, Shanghai, China, and the Ph.D. degree in 1995 from the University of Technology Sydney (UTS), Sydney, Australia, all in electrical engineering.

He was appointed a lecturer at UTS in 1994 and promoted to full professor in 2004 and Distinguished Professor of Electrical Engineering in 2017. At UTS, he has held various leadership positions, including the Head of School for School of Electrical, Mechanical and Mechatronic Systems and Director for Centre of Electrical Machines and Power Electronics. In 2018, he joined the University of Sydney, Australia, as a full professor and Head of School for School of Electrical and Information Engineering. His research interests include computational electromagnetics, measurement and modelling of magnetic properties of materials, electrical machines and drives, power electronics, renewable energy systems and smart micro grids.